



Ultrafast Facile One Pot Synthesis of Meso-Tetraphenyl-Porphinato–Cu(II) Metal–Organic Frameworks (MOFs) for CO₂ Capture

Khaled M. Elsabawy^{1,2} · Ahmed M. Fallatah²

Received: 27 March 2018 / Accepted: 7 July 2018 / Published online: 11 July 2018
© Springer Science+Business Media, LLC, part of Springer Nature 2018

Abstract

The present investigations introduce a new simple strategy to synthesize a crystalline copper metal–organic frameworks by high-energy He–Ag laser assisted synthesis for the first time in 18 min. The produced meso-tetraphenyl-porphinato–Cu(II) metal–organic frameworks (MOFs) were characterized by X-ray diffraction, scanning electron microscopy (SEM) and 3D-atomic force microscope (3D-AFM). Brunauer–Emmet–Teller BET specific surface area was measured and found 3418 m²g⁻¹. Furthermore meso-tetraphenyl-porphinato–Cu(II) metal–organic frameworks (MOFs) exhibit good sensitivity toward CO₂-capture with an adsorption capacity of 76.66 mg CO₂/g in 27.5 min at 25 °C, 40 bar.

Keywords Polymeric composite · Microstructure · Laser assisted · MOFs · 3D-AFM · CO₂-capture

1 Introduction

Crystalline metal–organic frameworks (MOFs) are considered one of the most important categories of porous materials, which find widespread in different types of applications including adsorption, gases-separation, catalysts, magnetism and some of pharmaceutical uses [1–5]. MOFs are typically constructed by connecting secondary building units (SBUs) with organic spacers to create diverse networks. Synthesis of metal–organic frameworks (MOFs) were performed by using different synthetic approaches as, solvothermal synthesis, microwave-assisted synthesis, electrochemical synthesis, mechanochemical synthesis and sonochemical synthesis [6–10].

2 Experimental

Meso-tetraphenylporphinato–Cu(II) was successfully synthesized via high energy He–Ag-laser assisted solvothermal procedures for the first time in 18 min as shown in Fig. 1a, the details of solvothermal synthesis procedures were described in [11].

The intensive energy absorbed via He–Ag laser (224.3 nm) irradiations is suffice to initiate and activate malonic acid linker in presence of DMF to close rings in the longitudinal axial direction as well as horizontally direction as clear in Fig. 1a, b forming 3D-MFOs.

2.1 He–Ag Laser Assisted Synthesis

The accurate molar ratios of copper nitrate trihydrate [Cu(NO₃)₂·3H₂O], tetraphenylporphinato ligand as well as malonic acid as organic linker were carefully dissolved in 120 ml of *N,N*-dimethylformamide (DMF) and sonicated for 10 min then, finally the container was subjected to be the target for He–Silver laser irradiations, with average power of 103 W cm⁻² at distance of 21 cm by angle 60°. The dose of irradiations was accumulated six times each of 3 min of irradiations with total accumulated time of 18 min.

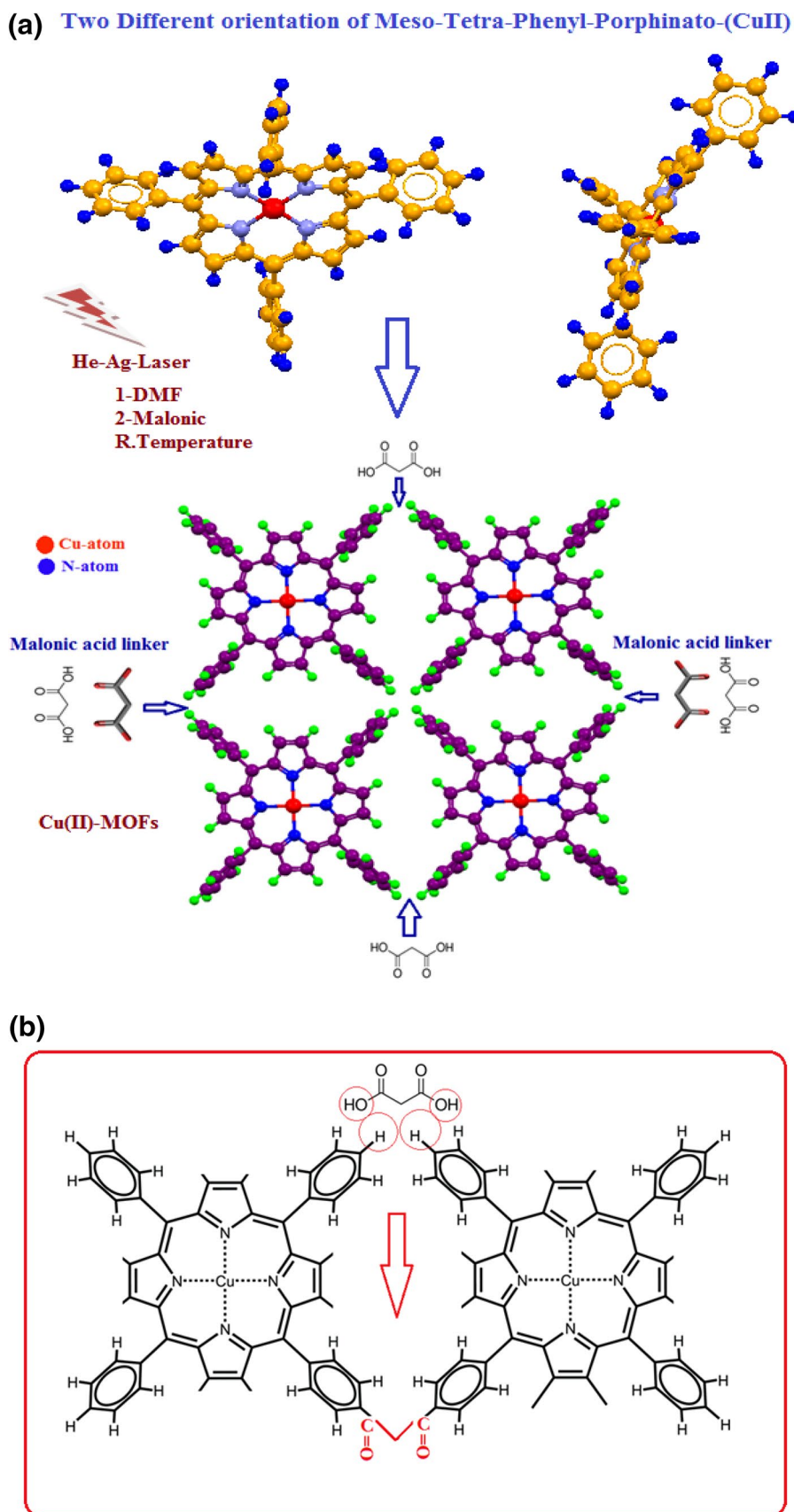
He–Silver laser has the following characteristics features, the laser output is insensitive to ambient temperature and requires no warm-up or other preheating and no temperature regulation. The laser head and power supply are designed

✉ Khaled M. Elsabawy
khaledelsabawy@yahoo.com; ksabawy@yahoo.com

¹ Materials Unit, Chemistry Department, Faculty of Science, Tanta University, Tanta 31725, Egypt

² Nano-Structured Materials Gp., Chemistry Department, Faculty of Science, Taif University, 888 Alhawya, Taif, Kingdom of Saudi Arabia

Fig. 1 **a** Schematic sequences of forming “Cu–MOFs” via laser assisted technique. **b** The final structure of Cu–MOFs showing the role of malonic acid linker. (Color figure online)



for operation at an average input power of 120 W in order to keep the system air cooled and simple. In order to provide the discharge conditions needed for optimum output (12 A at 350 V = 4.2 kW). The focal length F of the focusing lens, D is the beam diameter (5.5 mm), and λ is the laser wavelength (224.3 nm). Therefore this laser can be focused to 5 μm spot on sample with a 5.5 mm focal length.

3 Results and Discussions

3.1 Structural and Microstructural Features

The yield of meso-tetraphenylporphinato–Cu–MOFs was structurally investigated as it clear in Fig. 2a–e. The analyses of refined XRD pattern measured for laser assisted meso-tetraphenylporphinato–Cu–MOFs as shown in Fig. 2a were matched and compared with the crystalline data reported by Stevens [12] for tetragonal metallized-meso-tetraphenylporphinato complex where metal = cobalt. The evaluated lattice constants for meso-tetraphenylporphinato–Cu(II) (MOFs) were $a = b = 14.9770(4)$ and $c = 13.7434(4)$ Å, which are fully consistent with those reported by [12] for tetragonal phase with I-4 2d space group.

Figure 2b, c shows 3D-AFM tapping contact mode image for meso-tetraphenylporphinato–Cu–MOFs before and after forming MOFs. The surface topology analyses before laser irradiations shows heights gradient with maximum heights average of 1.26 μm while after laser assisted irradiations the surface topology has a lot of aggregated segregations on the surface and near to the surface's layers as a result of thermal effects of intensive ultra-high laser irradiations as reported by one of the authors themselves [13].

Figure 2d displays scanning electron micrograph captured for “Cu–MOFs” with average grains sizes ranged in between 1.1 and 3.8 μm as clear in Fig. 2d.

The molecular structure visualization and stability parameters of the “Cu–MOFs” were theoretically investigated by using diamond impact crystal program. The studies are concerned by stereo-orientations, crystal symmetry and torsion angles inside crystal lattice of “Cu–MOFs” as shown in Fig. 2e which represents space filling of meso-tetraphenylporphinato–Cu(II) molecule with extended internal stress.

Further more infrared absorption spectra measured for “Cu–MOFs” Fig. 2f confirmed the the presence of most functional groups in the proposed schemes Fig. 1a, b.

The molecular structure visualization studies indicated that, there are a two different orientations of tetraphenylporphinato–Cu complex as clear in Fig. 1, they are the main factor responsible for crystal stability of “Cu–MOFs”.

The (BET) specific surface area of laser assisted meso-tetraphenylporphinato–Cu–MOFs were carefully characterized by evaluating, Brunauer–Emmet–Teller (BET) specific surface areas with an automatic system (Model 2200A, Micro-meritics Instrument Co., Norcross, GA), by using nitrogen gas as an adsorbate at liquid nitrogen temperature as clear in Fig. 3a, b.

The BET surface area was found $\sim 3418 \text{ m}^2\text{g}^{-1}$ with large different pores sizes ranged in between “4–10.2 Å” which is ultrahigh value in contrast with ordinary adsorbents or carbon based materials [14, 15].

3.2 CO₂-Capture Experiment

For checking sensitivity of laser assisted Cu–MOFs with ultrahigh BET-surface area $\sim 3418 \text{ m}^2\text{g}^{-1}$ towards “CO₂” capture, kinetic investigations were performed via fully automated Sievert-type Apparatus as shown in Fig. 4. The curve of pressure composition isotherm (PCI) were performed inside gas reaction controller (GRC) with PCI adsorption Mode (PC1a).

The activation of 1 g of Cu–MOF was performed via 100 ml methanol solution at 60 °C for 24 h, the methanol solution was replaced each 8 h to swell porous Cu–MOF as possible to be applicable in the CO₂-isotherm capture experiment.

As it clear in Fig. 4 the kinetics of adsorption (uptake CO₂) were very fast in the first 10 min with ratio of 65.27% from maximum adsorption capacity which was 76.66 mg CO₂/g of “Cu–MOFs” as shown in Fig. 4. The adsorption experiment was performed for 70 min while the maximum adsorption loading was achieved after only 27.5 min with adsorption capacity of 76.66 mg CO₂/g which is considered a promising result in contrast with some others MOFs adsorbents materials [14, 15].

The present laser assisted “Cu–MOFs” has BET surface area of $\sim 3418 \text{ m}^2\text{g}^{-1}$, which is relatively high value and can be compared with some of common known MOFs. For example, MOF-210 is the highest surface area (10,450 m^2g^{-1}) MOF known to date, constructed from 4,4,00-[benzene-1,3,5-triyl-tris(ethyne-2,1-diyl)]tribenzoate (H3BTE), biphenyl-4,40-dicarboxylate (H2BPDC), and zinc(II)nitrate hexahydrate [16]. Other well known MOFs, such as NU-100 (69.8 wt%, 40 bar at 298 K), Mg–MOF-74 (68.9 wt%, 36 bar at 278 K), MOF-5 (58 wt%, 10 bar at 273 K), and HKUST-1 (19.8 wt%, 1 bar at 298 K), also show good sensitivity for “CO₂” uptake [17, 18].

Furthermore the present Cu–MOFs can be compared with some new MOFs as reported in [19–21] specially on the point of view “CO₂” capture. Li et al. [19] reported on the

XRD-Pattern for Tetragonal Cu-MOF with I-42d Space Group

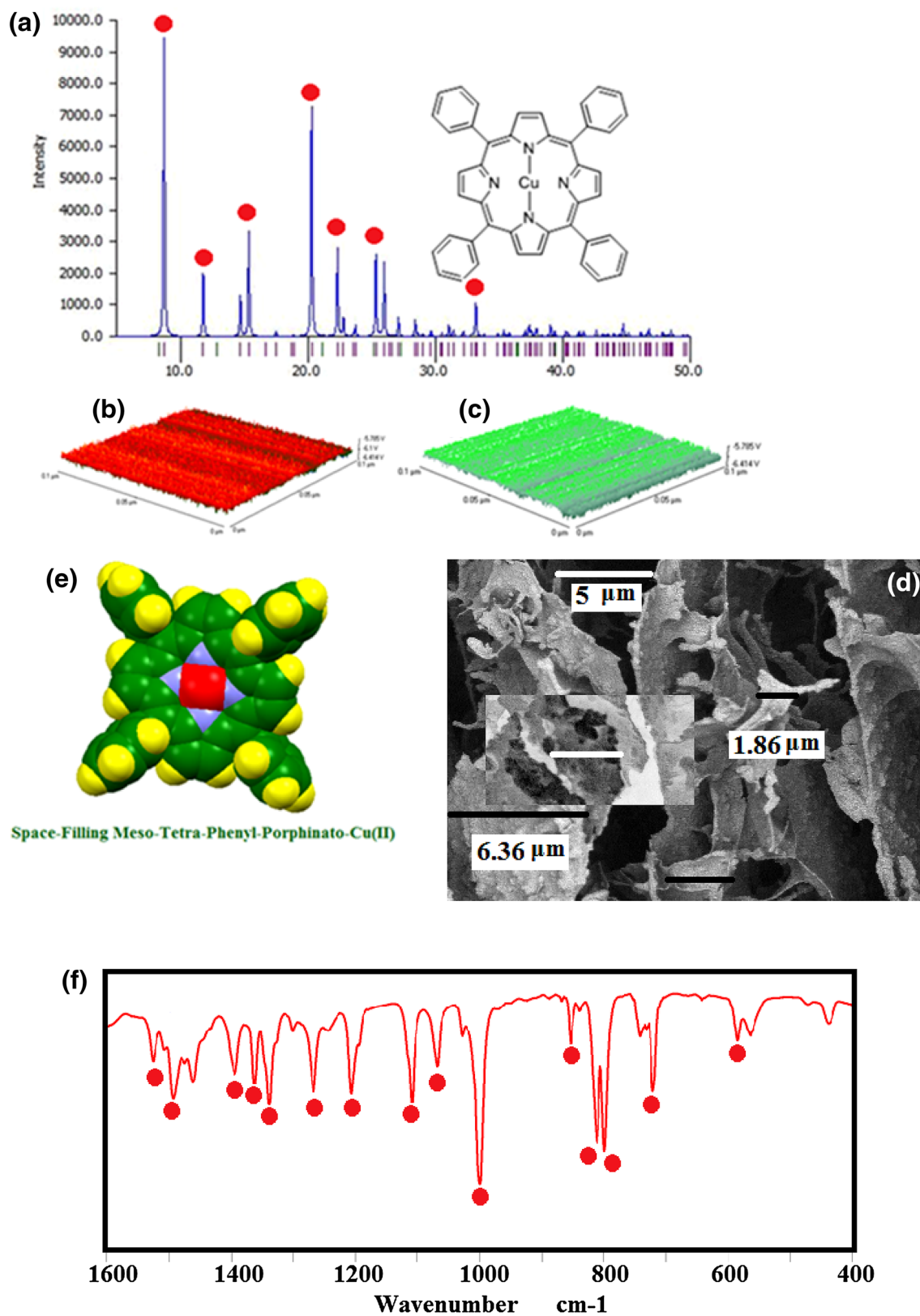


Fig. 2 a–e Different structural measurements measured for synthesized laser-assisted meso-tetraphenylporphinato–Cu(II) (MOFs); **a** XRD-pattern, **b** 3D-AFM-for meso-tetraphenylporphinato–Cu–MOFs before laser assisted irradiations, **c** 3D-AFM-for meso-tetraphenylporphinato–Cu–MOFs after laser irradiation process and forming of MOFs, **d** SE-micrograph for Cu–MOFs, **e** Space filling of meso-tetraphenylporphinato–Cu molecule. For **d** micron scale bar = 5 μm . **f** Infrared absorption spectra measured for Cu–MOFs

first strontium-based MOF possessing polar tubular channels for CO_2 and C_2H_6 capture while, Wang et al. [20] and Hou et al. [21] introduced new cobalt based and advanced rod packing MOFs as high selective MOFs for “ CO_2 ” capture.

On the other hand these results can be compared with those reported by Goel [22] who investigated, two new Cu- organic frameworks and checked them as H_2 and N_2 trappers.

The present copper–MOFs exhibited good sensitivity to CO_2 capture with reasonable adsorption uptake capacity of $\sim 76.66 \text{ mg CO}_2/\text{g}$ and in the near advance it will be checked as toxic gases sensors. Some of Tb–MOFs were successfully applied as selective sensor of picric acid among nitro-aromatic explosives through fluorescence quenching mechanism, acetone and tri-nitro-phenol (TNP) [23, 24].

4 Conclusions

As a summary the present studies are introducing a new approach with eco-strategy to synthesize Cu–MOFs with ultrahigh specific surface area ($\sim 3418 \text{ m}^2\text{g}^{-1}$) by applying

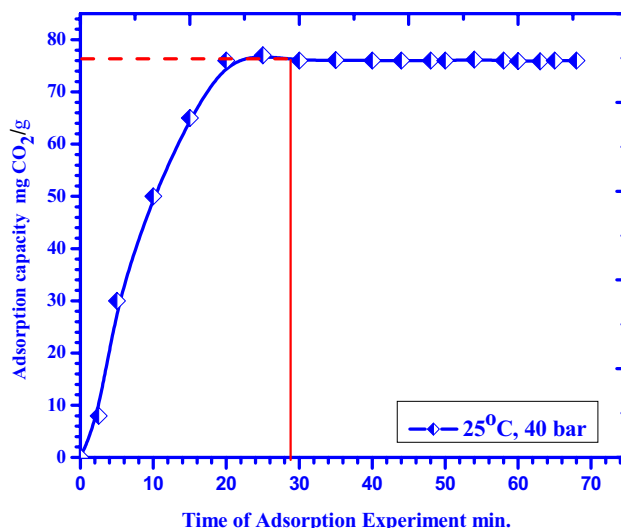


Fig. 4 Adsorption/time curve for 1 g sample of Cu–MOFs at 25 °C, 40 bar CO_2

high energy He–Ag laser for the first time. The produced copper–MOFs exhibited good sensitivity to CO_2 capture with reasonable adsorption uptake capacity of $\sim 76.66 \text{ mg CO}_2/\text{g}$. The synthesized Cu–MOFs has ultrahigh surface area but evaluated pore sizes not unified which due to that the rate of Cu–tetraphenylporphinato–MOFs 3D-growth not regular through axial and horizontal directions.

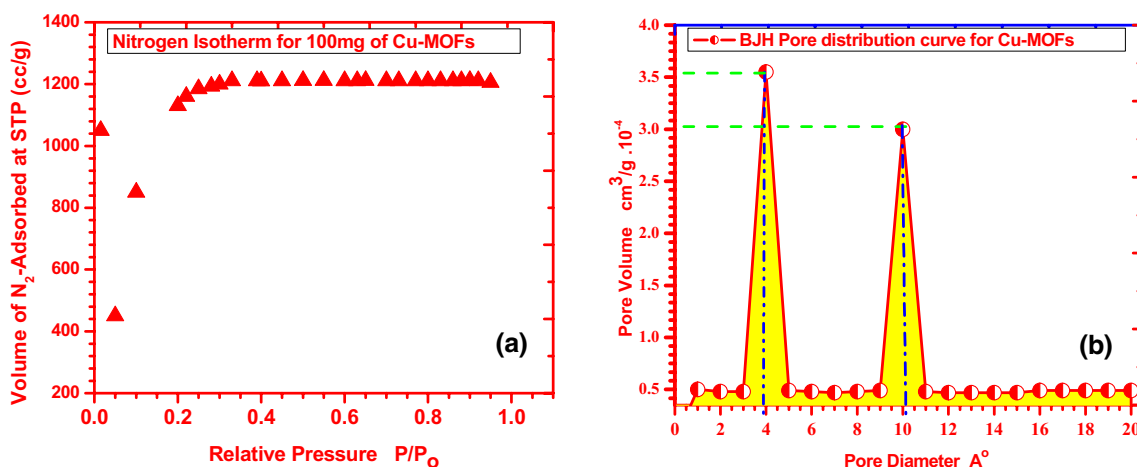


Fig. 3 a N_2 -isotherm curves applied for 100 mg of Cu–MOFs and **b** BJH-pore distribution curve of Cu–MOFs

References

1. H.C. Zhou, J.R. Long, O.M. Yaghi, Introduction to metal–organic frameworks. *Chem. Rev.* **112**, 673–674 (2012)
2. A.U. Czaja, N. Trukhan, U. Muller, Industrial applications of metal–organic frameworks. *Chem. Soc. Rev.* **38**, 1284–1293 (2009)
3. N. Stock, S. Biswas, Synthesis of metal–organic frameworks (MOFs). *Chem. Rev.* **112**, 933–969 (2011)
4. H.K. Chae, D.Y. Siberio-Pérez, J. Kim, Y. Go, M. Eddaoudi, A.J. Matzger, M. O’Keeffe, O.M. Yaghi, A route to high surface area, porosity and inclusion of large molecules in crystals. *Nature* **427**, 523–527 (2004)
5. D.J. Tranchemontagne, Z. Ni, M. O’Keeffe, O.M. Yaghi, Reticular chemistry of metal–organic polyhedral. *Angew. Chem. Int. Ed.* **47**, 5136–5147 (2008)
6. C. Wang, J.Y. Ying, Sol–Gel synthesis and hydrothermal processing of anatase and rutile titania nanocrystals. *Chem. Mater.* **11**, 3113–3120 (1999)
7. A. Lagashetty, V. Havanoor, S. Basavaraja, S.D. Balaji, A. Venkataraman, Microwave-assisted route for synthesis of nanosized metal oxides. *Sci. Technol. Adv. Mater.* **8**, 484–493 (2007)
8. A.M. Joaristi, J.J. Alcan, P.S. Crespo, F. Kapteijn, J. Gascon, Electrochemical synthesis of some archetypical Zn²⁺, Cu²⁺, and Al³⁺ metal organic frameworks. *Cryst. Growth Des.* **12**, 3489–3498 (2012)
9. T. Friscic, I. Halasz, P.J. Beldon, A.M. Belenguer, F. Adams, S.A. Kimber, V. Honkima, R.E. Dinnebir, Real-time and in situ monitoring of mechanochemical milling reactions. *Nat. Chem.* **5**, 66–73 (2013)
10. J. Kim, S. Yang, S.B. Choi, J. Sim, J. Kim, W. Ahn, Control of catenation in CuTATB-*n* metal–organic frameworks by sonochemical synthesis and its effect on CO₂ adsorption. *J. Mater. Chem.* **21**, 3070–3076 (2011)
11. E.D. Dikio, A.M. Farah, Synthesis, characterization and comparative study of copper and zinc metal organic frameworks. *Chem. Sci. Trans.* **24**, 1386–1394 (2013)
12. E.D. Stevens, Electronic structure of metalloporphyrins. 1. Experimental electron density distribution of (meso-tetraphenylporphinato) cobalt(II). *J. Am. Chem. Soc.* **103**, 5087 (1981)
13. K.M. ElSabawy, M.H. El-Newehy, Pulsed-Nd-laser irradiations effects on structural and micro-structural features of optimally lutetium thorium-codoped free lead-2212-BSCCO. *Appl. Surf. Sci.* **258**, 1345–1352 (2011)
14. W.K. Son, J.H. Youk, W.H. Park, Electrospinning of cellulose acetate in solvent mixture *N,N*-dimethylacetamide (DMAc)/acetone. *J. Polym. Sci. B* **42**, 5 (2004)
15. F. Xu, Z. Tang, S. Huang, L. Chen, Y. Liang, W. Mai, H. Zhong, R. Fu, D. Wu, Facile synthesis of ultrahigh-surface-area hollow carbon nanospheres for enhanced adsorption and energy storage. *Nat. Commun.* **6**, 7221 (2015)
16. H. Furukawa, N. Ko, Y. B. Go, N. Aratani, S.B. Choi, E. Choi, A.O. Yazaydin, R.Q. Snurr, M. O’Keeffe, J. Kim, O.M. Yaghi, Ultra-high porosity in metal–organic frameworks. *Science* **329**, 424–428 (2010)
17. A.G.W. Foy, A.J. Matzger, O.M. Yaghi, Exceptional H₂ saturation uptake in microporous metal–organic frameworks. *J. Am. Chem. Soc.* **128**, 3494–3495 (2006)
18. G. Férey, C.M. Draznieks, C. Serre, F. Millange, J. Dutour, S. Surble, I. Margiolaki, A chromium terephthalate-based solid with unusually large pore volumes and surface area. *Science* **309**, 2040–2042 (2005)
19. X.Y. Li, Y.Z. Li, Y. Yang, L. Hou, Y.Y. Wang, Z. Zhu, Efficient light hydrocarbon separation and CO₂ capture and conversion in a stable MOF with oxalamide-decorated polar tubes. *Chem. Commun.* **53**, 12970–12973 (2017)
20. H.H. Wang, L. Hou, Y.Z. Li, C.Y. Jiang, Y.Y. Wang, Z. Zhu, Porous MOF with highly efficient selectivity and chemical conversion for CO₂. *ACS Appl. Mater. Interfaces* **9**(21), 17969–17976 (2017)
21. L. Hou, W.J. Shi, Y.Y. Wang, Y.G.C. Jin, Q.Z. Shi, A rod packing microporous metal–organic framework: unprecedented *ukv* topology, high sorption selectivity and affinity for CO₂. *Chem. Commun.* **47**, 5464–5466 (2011)
22. N. Goel, Study of new Cu(II) metal–organic frameworks: syntheses, structural, gas sorption and magnetic properties. *Inorg. Chim. Acta* **450**, 330–336 (2016)
23. N. Goel, N. Kumar, A stable nonanuclear Tb(III) cluster for selective sensing of picric acid. *Inorg. Chim. Acta* **463**, 14–19 (2017)
24. N. Goel, N. Kumar, A dual-functional luminescent Tb(III) metal–organic framework for the selective sensing of acetone and TNP in water. *RSC Adv.* **8**, 10746 (2018)